Realism of Tactile Texture Playback: A Combination of Stretch and Vibration

Zhenyu Liu, Jin-Tae Kim, John A. Rogers, *Fellow, IEEE*,
Roberta L. Klatzky, *Fellow, IEEE*, and J. Edward Colgate, *Fellow, IEEE*

***Abstract*—This study investigates the effects of two stimulation modalities (stretch and vibration) on natural touch sensation on the volar forearm. The skin-textile interaction was implemented by scanning three natural textures across the left forearm. The resulting in-plane displacements across the skin were recorded by the digital image correlation technique to capture the information imparted by the textures. The texture recordings were used to create three playback modes (stretch, vibration, and both), which were reproduced on the right forearm. Two psychophysical experiments compared the physical texture scans to rendered texture playbacks. The first experiment used a matching task and found that to maximize perceptual realism, i.e., similarity to a physical reference, subjects preferred the rendered texture to have a playback intensity of approximately 1X – 2X higher on DC components (stretch), and 1X – 3.5X higher on AC components (vibration), varying across textures. The second experiment elicited similarity ratings between the texture scans and playbacks and showed that a combination of both stretch and vibration was required to create differentiated texture sensations. However, the intensity amplification and use of both stretch and vibration were still insufficient to create fully realistic texture sensations. We conclude that mechanisms beyond single-site uniaxial stimuli are needed to reproduce realistic textural sensations.**

***Index Terms*—Forearm perception, texture playback, stretch, vibration, digital image correlation.**

I. Introduction

When we engage in exploration and manipulation of our surroundings, relative motion is generated between the skin and contact surface, resulting in complex mechanical interactions within and surrounding the contact patches [1]–[3]. These mechanical responses are converted into peripheral nerve action potentials by multiple mechanoreceptors to yield the perception of surface texture [4]. Previous studies revealed a duplex mechanism of perception, whereby tactile sensations are influenced by both spatial deformation and temporal responses on the skin [5], [6]. Correspondingly, haptic feedback, which enhances users' interactions with computers and other input/output systems, can be achieved through vibration, pressure, stretch, and other proprioceptive and directional cues [7].

Depending on which part of the body is being stimulated, whether glabrous skin or hairy skin, the same stimulus can produce different perceptual outcomes. Whether coded spatially or temporally, the high-bandwidth information associated with textural variations is better conveyed in glabrous skin of fingers and palms, which is densely innervated with mechanoreceptors. It has been shown that fingertips are one of the most sensitive areas on the body [8]. Considering vibratory coding in particular, the detection thresholds on hairy skin are reported as significantly higher than those on glabrous skin [9]. This difference has resulted in most texture-based research being focused on the finger and palm [2], [10]–[12]. In contrast, haptic displays deployed on hairy skin are more practical in scenarios such as physical therapy, prosthetics manipulation, sports training, etc. [13]. Correspondingly, body-mounted haptic interfaces have been developed and are able to provide stimuli on hairy skin [7], [14]–[16]. However, the fundamental understanding of haptic feedback on hairy skin remains incomplete, and recreating realistic sensations on the hairy skin is still challenging. In addition to the technical challenges of reproduction of stimulation on insensitive skin, difficulties of modeling skin-texture contact remain unsolved.

The mechanical response of skin during interaction with textures can be attributed to at least two types of stimuli: high-frequency vibration caused by texture microgeometry and low-frequency stretch caused by contact friction. Currently, the main stimulation mode for tactile interfaces is vibration. Compact vibrotactile actuators can deliver rich information by changing the amplitudes and frequencies of actuation, achieving high perceptibility. However, the different properties between the two types of skin make the vibratory stimuli applied on the hairy skin less effective. Aside from vibratory stimuli, low-frequency skin stretch also provides important tactile information and has been exploited in compact and low-power wearable devices [17]. Nonetheless, low-bandwidth stretch of hairy skin is not as information-dense as vibration. Combining the advantages of both types stimuli, a multi-modal wearable device may provide more possibilities for haptic perception.

Regarding glabrous skin, both Wiertlewski *et al.* [10] and Grigorii *et al.* [12] have demonstrated that a single stimulation mode was insufficient for creating real texture sensations on the fingertip. For hairy skin, existing studies have mainly concentrated on a single stimulation mode (stretch or vibration). Sullivan *et al.* [18] integrated skin stretch and vibrotaction

Corresponding author: Zhenyu Liu.

Zhenyu Liu and J. Edward Colgate are with the Department of Mechanical Engineering, Northwestern University, Evanston, IL 60208, USA (email: zhenyuliu2021@u.northwestern.edu; colgate@northwestern.edu).

Jin-Tae Kim is with the Querrey Simpson Institute for Bioelectronics, Northwestern University, Evanston, IL 60208, USA, and the Department of Mechanical Engineering, Pohang University of Science and Technology, Pohang 37673, Republic of Korea (email: jin.kim4@northwestern.edu).

John A. Rogers is with the Department of Materials Science and Engineering and the Querrey Simpson Institute for Bioelectronics, Northwestern University, Evanston, IL 60208, USA (email: jrogers@northwestern.edu).

Roberta L. Klatzky is with the Department of Psychology, Carnegie Mellon University, Pittsburgh, PA 15213, USA (email: klatzky@cmu.edu).

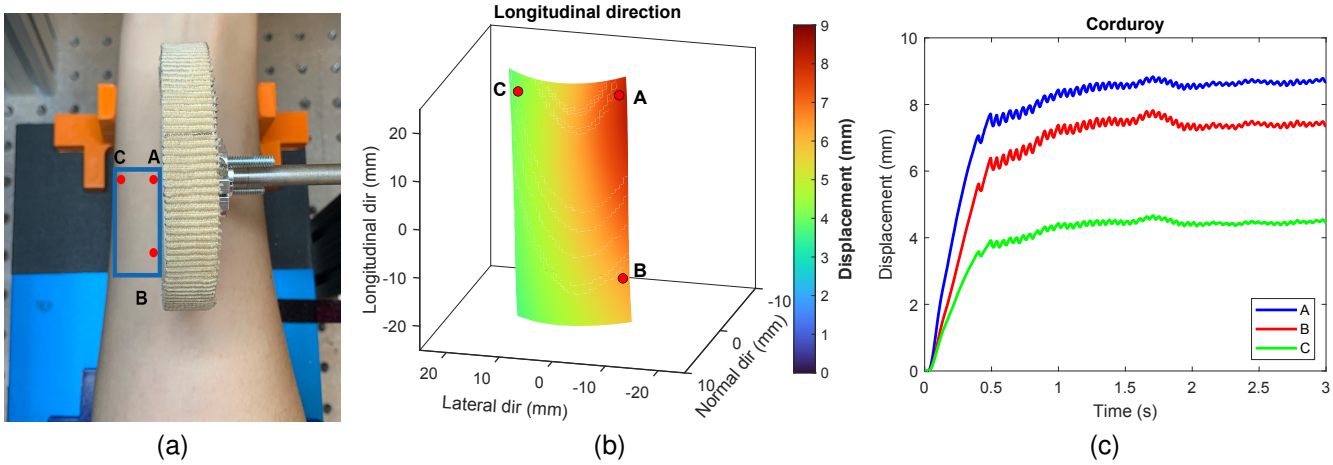

Fig. 1. (a). Measuring area of the 3D-DIC method. Three test points within this area were selected. (b). 3D-DIC results for scanning corduroy. It shows the skin displacements in the longitudinal direction at the time of 3 s. (c). Longitudinal displacements of three test points versus time.

into the wearable haptic interface and found that cue distinguishability was higher when both stimuli were present, simply owing to more available cues. However, similar to Sullivan *et al.*'s work, most research focusing on hairy skin perception investigates the tactile distinguishability or proprioceptive feedback via simple stimuli [19]–[21], instead of seeking to create realistic sensations of textures. Therefore, the interaction between stretch and vibration, and their contribution to the realism of texture playback, remain to be investigated.

In this study, we simulated the skin-textile interaction on the volar forearm and measured two types of mechanical responses (stretch and vibration) as skin displacements. By reproducing three modes of playback on the forearm (stretch, vibration, and both), our study evaluates the performance of different playback modes and concludes that combining two types of stimuli can recreate differentiated texture sensations more effectively.

II. Methods

A. Preliminary Experiment: Measuring Skin Responses

Experiments and analyses are complex due to the forearm skin's nonlinearity, anisotropy, and viscoelasticity [22]. To evaluate the skin mechanical responses on the skin elicited by the texture scan, a preliminary experiment was conducted on the experimenter (male, 25) by scanning several natural textures on his right forearm using a rotating wheel at a constant speed. Each selected texture was scanned once along the longitudinal direction (from elbow to wrist). To measure the overall skin responses and minimize the effect of measurement technique on the skin properties, a non-contact approach, the three-dimensional digital image correlation (3D-DIC) method, was used in our experiment. As the contact area directly under the wheel was not visually available, an adjacent rectangular measuring area was designated to represent the mechanical responses of the contact patch (Fig. 1a).

Two high-speed cameras (HT-2000M, Emergent Vision Technologies, Canada) were used for capturing the videos of the designated area at a sampling frequency of 500 Hz. Prior to the experiments, the measuring area on the forearm was shaved and evenly covered with water-based black spray paint (Fantasy FX^{TM} Makeup, Mehron, Chestnut Ridge, NY) to generate randomly distributed speckle patterns. The measuring area was approximately 40 mm in the longitudinal direction and 15 mm in the lateral direction. 3D displacements were obtained by processing the captured videos with an open-source 3D-DIC software MultiDIC [23] using the same configuration as Kim *et al.*'s study [24].

Texture selection. Our selection of textures was constrained by the relatively high detection thresholds for vibration on hairy skin at the forearm, which means that substantial textural differences are required to allow ease of discrimination [9]. As such, textures that have similar microgeometries (e.g. denim and canvas) cannot be easily differentiated on the forearm. Preliminary experiments also excluded smooth fabrics such as velveteen, as they did not elicit sufficient skin responses. Therefore, three textile samples with different periodic microgeometries were chosen for our study (Fig. 2). To generate corresponding topographical profiles, the selected textile samples were scanned by a high-resolution stylus-based profilometer (Dektak 150, Bruker, Billerica, MA).

Results: Directional displacement. The 3D-DIC results showed that the displacements in the longitudinal direction (Fig. 1b) were approximately 10 and 16 times larger than those in the lateral and normal directions respectively. As such, further studies only included displacements in the longitudinal

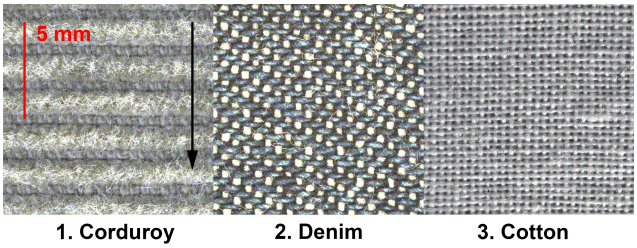

Fig. 2. Selected textures used in the studies, ordered by decreasing surface topographical heights. The arrow indicates the scan direction.

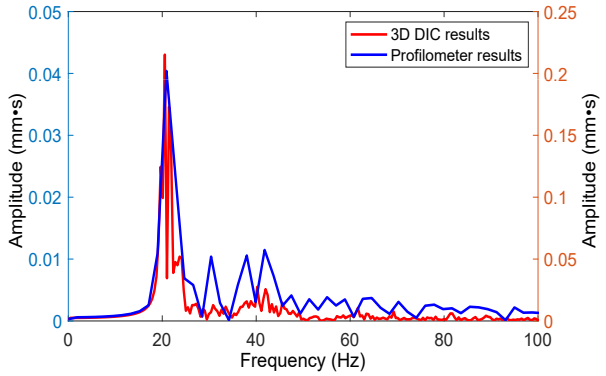

Fig. 3. 3D-DIC results and the profilometer data of corduroy, presented as the frequency spectra. Only AC components were considered, and low-frequency components under 20 Hz were filtered.

direction to represent the mechanical responses of skin. The longitudinal displacements on different locations within the measuring area were highly correlated and synchronized, while the amplitudes varied widely. In order to evaluate the decay of skin responses with distance along different directions, three points (A, B, and C) within the measuring area were selected as test points, as shown in Fig. 1a and 1b. A and B were adjacent to the contact patch and had the same lateral coordinate, while A and C had the same longitudinal coordinate as the projected coordinate of the wheel shaft.

Results: DC and AC modes. The displacements of the three test points for scanning corduroy are shown in Fig. 1c. The full texture scan can be divided into two stages: skin stretch (DC components only) and high-frequency vibrations while stretch persists (AC components with constant DC components). In the first stage, negligible relative movement occurred between the texture and the skin, and there was an approximately linear relationship between time and displacement. The forearm skin was longitudinally stretched from the initial position, and the skin stretch was represented by the DC component in the displacement. In the second stage, the pre-stretched skin was mainly affected by two types of in-plane forces: the friction owing to skin-texture interaction and the skin elastic force, both of which changed dynamically during the texture scan. The directions of these two forces were 180 degrees apart. When the friction was greater, the skin and the texture were relatively stationary and appeared to be stuck together. On the contrary, when the elastic force was greater, the skin slipped towards the opposite direction of the texture scan, i.e., towards its initial position. As a result, the stick-slip motion occurred at the skin-texture interface, corresponding to vibration on the skin that appeared as the AC component in the displacement. It can be noticed from Fig. 1c that within the measuring area, both DC and AC components decline rapidly in the lateral direction while decreasing slightly in the longitudinal direction.

Skin-texture friction can be derived from the magnitude of the DC component of skin stretch, which was found to correlate well with each texture's respective topographical heights based on the profilometer measurements. For the AC components, the DIC results of the three textures and the corresponding profilometer data also matched (an example is shown in Fig. 3), indicating that skin vibration was primarily influenced by the microgeometry of the texture. The frequency of the skin vibration (AC components) can be expressed as

$$f_t = \frac{v_s}{\lambda_t} \tag{1}$$

where f_t is the temporal frequency of the texture in Hz, v_s is the scanning speed in mm/s, and λ_t is the wavelength in mm.

B. Texture Recorder and Player

In further experiments, we sought to record skin-textile interaction on one forearm and play it back on the other. To implement the skin-textile interaction, three textile samples were scanned across the volar forearm at a constant speed along the longitudinal direction. Longitudinal movement allowed for a more comfortable experience for the participants than lateral movement, and resulted in a more accurate perception of stimuli directions as well as amplitudes [25]. Additionally, studies have demonstrated that the forearm is more sensitive to tangential forces than normal ones and can differentiate the direction of skin stretch through displacements as small as 0.13 mm [17], [26]–[28].

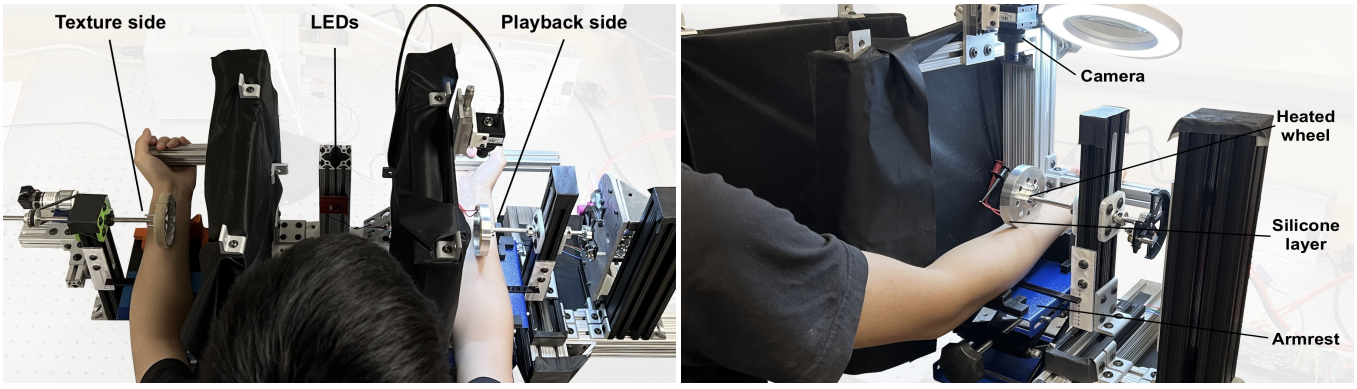

Fig. 4. Apparatus overview. (a). Top view with the DIC setup on the playback side. (b) The view of the playback side.

Accordingly, a pair of rotating wheel stimulators was customized to achieve texture scans and playbacks on the left and the right forearms respectively (Fig. 4). A left-right mirrored design was used to maximize the similarity between the two sides, except for the actuation mechanisms. On the texture side, each texture sample was affixed to a polylactic acid (PLA) wheel via a spray adhesive (Super 77^{TM}, 3M, St Paul, MN). The wheels were 76.2 mm in diameter and 12.7 mm thick to ensure firm contact with the forearm. To actuate the texture scans, the texture-coated PLA wheel was rotated by a brushed DC motor (415A832, Globe Motors, Dayton, OH) via a timing belt transmission, and the scanning speed at the skin-texture interface was maintained at 40 mm/s. The motor was equipped with a 187.68:1 step-down gearbox to change the output torques. To ensure the texture-elicited skin displacements were not obscured by vibrations created by the motor, we verified that the motor and wheel generated negligible vibrations during rotation by scanning a bare wheel on the forearm and measuring the skin displacements.

On the playback side, to eliminate perceptual differences as much as possible, the wheel and the armrest had the same sizes as the texture-scan side. The wheel was made from aluminum and heated with flexible heaters (DR1008-2.5, Birk Manufacturing, East Lyme, CT) to eliminate possible thermal cues. Additionally, the wheel was covered with a 500 μm layer thick of sticky silicone (Ecoflex^{TM} 00-10, Smooth-On, Macungie, PA) to eliminate the relative movements between the skin and the wheel. To recreate the low-frequency stretch and high-frequency vibrations very similar to the ones elicited by the natural textures, the wheel on the playback side was driven by a brushless DC motor (EC60-614949, Maxon, Switzerland) via capstan transmission. Opaque black fabric was used on both sides to block the apparatus from view.

Before the experiments, subjects were seated at a workbench in front of the apparatus where they placed each arm in the setup and were allowed to make ergonomic adjustments such that both arms would be in a relaxed position to minimize any involuntary movements. The height of the armrest on both sides was adjusted till a normal load of 0.5 N was applied. This was measured via a force-sensitive resistor (FSR^{TM}400, Interlink Electronics, Camarillo, CA) at the contact interface. The experiments were started immediately after adjustment to minimize the effect of skin indentation. Each texture scan and playback lasted 3 seconds. After each trial, the height of the armrest was reset to release the stretched skin. The experimental processes were aided by two LEDs in front of the subjects, which indicated whether the real or rendered texture was being presented.

C. Texture Recording and Playback

Based on the preliminary experiment, we recorded only the longitudinal displacements for each texture and rendered the corresponding playbacks on the volar forearm. The 2D-DIC method was utilized to record the texture-elicited skin responses more efficiently. A single camera (DFK 37BUX273, The Imaging Source, Charlotte, NC) was used to record the videos of the designated area. Other experimental conditions remained the same as the ones in the preliminary experiment. Pilot studies for recording skin responses were conducted on six subjects. It was verified that the temporal aspects of the DIC data were quite similar across subjects, although the amplitudes were variable. Based on this, and to streamline data collection, further recordings were done with only the experimenter's left forearm, and amplitude adjustment was incorporated into the psychophysical experiments. For each instance of texture recording via the DIC method, the time of pure stretch (DC components), the frequency of the vibration (AC components), and the amplitudes of DC and AC components on the skin were recorded. The recording of each texture was repeated five times to get the average values for enhancing measurement precision (TABLE I).

TABLE I
DIC VALUES OF TEXTURE RECORDING

Texture	Corduroy	Denim	Cotton
DC Time (s)	0.23	0.12	0.1
DC Amplitude (mm)	7.3	5.7	4.5
AC Frequency (Hz)	21	42	90
AC Amplitude, Peak Value (mm)	0.1	0.04	0.02

After collecting the 2D-DIC signals, we sought to create the texture playback. Since the DIC data in each individual texture recording exhibited a certain degree of randomness and were easily influenced by involuntary movements, using filtered DIC results as the input for playback proved quite challenging. Instead, we found that the longitudinal displacements on the skin could be represented by a concatenation of two simple waveforms with specific amplitudes and frequencies.

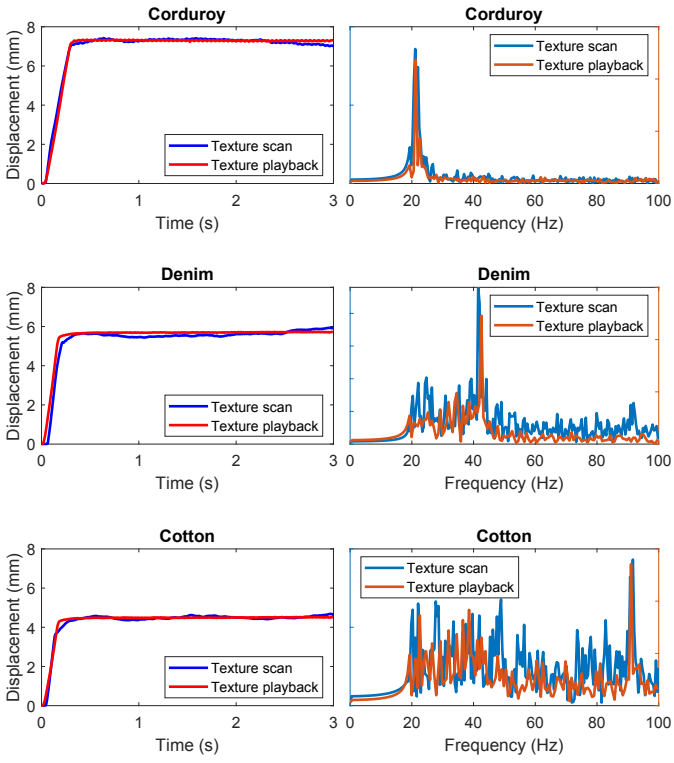

Fig. 5. Signals of texture scan and playback in the time domain and the spectra of their AC components.

First was pure stretch, which was constructed from a ramp waveform, and second was vibration which was constructed from a triangle waveform. The triangle waveform was made asymmetric in accordance with the stick-slip motion. The three playback modes of each texture scan were generated by these two components, and the motor was driven via close-loop position control (Fig. 5).

During the measurement process, the subject put both forearms on the armrests and felt the texture scan and playback simultaneously. The measuring areas designated on both volar forearms were symmetric. The longitudinal displacements of both measuring areas were recorded via the 2D-DIC technique. Considering the measuring areas as 2D planes, we chose one point on each side (the same location as point A in Fig. 1a and its mirrored location on the other side) as the test points for comparison. These points were adjacent to the contact patches in the lateral direction to minimize signal degradation due to the vibration propagation across the skin. Unless otherwise noted, all the test points in this study had the same longitudinal coordinate as the projected coordinate of the wheel shaft.

Both the displacements of the texture scans and playbacks (in the "both" mode) are displayed in Fig. 5. In verifying the accuracy of the playback, frequencies under 20 Hz in the AC component were filtered out owing to the involuntary movements of individuals and noise. It is apparent from the figure that the longitudinal skin stretch and vibration on the left forearm have been accurately reproduced on the right forearm. Additional tests further confirmed that displacements of different points are highly correlated, which means that if one point is tracking precisely, the other points are tracking accurately as well. To assess the performance of the three modes, two psychophysical experiments were designed and conducted.

D. Psychophysical Experiments

A total of fourteen subjects (aged 28.75 $\pm$ 6.79 years, six females) participated in the two experiments. The experimental protocol was approved by the Northwestern University Institutional Review Board. All subjects gave their written consent and received financial compensation for their time spent in the experiments. Subjects reported no physical or cognitive impairment nor any pathology that might interfere with the results. Prior to the experiments, subjects were asked to wash both of their forearms with soap and warm water and dry them with paper towels. The subjects wore noise-canceling headphones that played pink noise throughout the experiments to mask any possible audio cues generated by the apparatus. The average time for the two psychophysical experiments was approximately 60 mins.

1) Experiment 1: Previous studies have demonstrated that skin responses vary among individuals due to the differences in skin properties. To find the optimal similarity of sensations between the texture scan and playback for each individual, subjects were tasked with adjusting the gains of DC and AC components in a 2D parameter space, where the axes were the DC and AC gains. The unity gain case corresponded to the physical (2D-DIC) data. The optimal location in this space indicated the optimal perceptual match. Similar to a previous study [29], a guided exploration test was adapted to help subjects explore the space with several comparisons and find the optimal gains. Initially, the subjects put both their forearms on the armrests in relaxed positions and gently held the handles. They then felt a scanned texture on one arm, followed by two playback textures. After that, they orally reported the playback that better matched the actual texture, or said "unsure". The successive choices were generated by an algorithm that, with the characteristics of the gradient descent and the Nelder-Mead method [30], utilized the subjects' comparison answers to reduce the radius of the search region iteratively until an optimal point was reached. Specifically, four pairs of vectors were generated during each iteration, based on the current location and search radius. Two vectors in each pair had the same magnitude but opposite directions. The playback choices given to subjects required them to choose one direction or report "unsure", meaning that neither was chosen. The decisions for the four pairs determined the location in the next iteration, when the search radius would decrease. Each assessment had three iterations, after which the optimum playback gains were identified. By connecting the locations in each iteration sequentially, a trajectory in the 2D parameter space could be generated. The number of iterations was established with preliminary tests that indicated the endpoints did not change substantially beyond the third iteration. This trial was repeated three times, each with a different starting point in the parameter space. The experiment was repeated for each of the three textures. Subjects were not constrained in the time to make decisions and could feel both stimuli repeatedly upon request. The textured wheels were changed manually by the experimenter when guided exploration for one texture was finished.

2) Experiment 2: Subjects were presented simultaneously with a physical texture scan and a playback. They were asked to rate the similarity of the pair on a Likert scale of 1 to 9 (1 = "completely dissimilar", 9 = "almost identical sensation", and 5 = "moderately similar"). The texture playback was drawn from three textures: corduroy, denim and cotton, and each of the playback textures was tested on separate trials with each of the three playback modes: 1) skin stretch only, 2) vibration only, 3) both skin stretch and vibration. In the stretch mode, the wheel pushed the skin longitudinally to the preset position and kept still. In the vibration mode, the wheel vibrated back and forth, applying a constantly changing tangential force to the skin. The "both" mode combined stretch and vibration. The amplitudes of playbacks were scaled with the optimal gains each subject chose in the first experiment. The nine playbacks (three playback modes, three textures per mode) were presented in random order in conjunction with a single physical texture. The physical textures were presented in counterbalanced order across subjects, who were allowed to take breaks to prevent fatigue.

E. Supplementary Experiment

A supplementary experiment was performed to investigate mechanical interactions between skin stretch and vibration amplitude, which might have affected perception. The playbacks

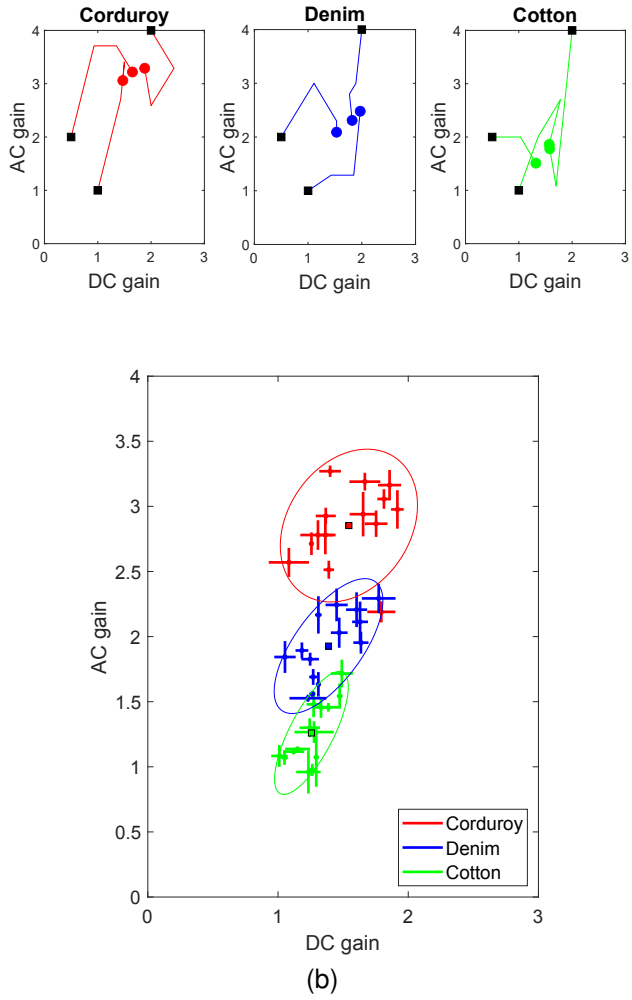

Fig. 6. (a). Trajectories of guided exploration test for one subject. Black squares indicate the start points and circles indicate the endpoints. (b). Distribution of gains for 14 subjects with 95% confidence ellipses. Each cross represents one subject's three responses, centered on the mean. The squares indicate the centers of the ellipses, i.e., the central trend across subjects.

of three textures in the "both" mode were presented on the experimenter's right forearm. The desired deformation on the skin (texture playback) was equal to the gain multiplied by the physical data (texture recording). Using a constant AC gain of 1.0, the DC gain was adjusted from 0 to 1.0 with a step size of 0.2. A value of 0 indicates no stretch and 1.0 indicates the same DC amplitude as the physical texture scan. Records from the motor encoder indicated that the output vibration remained constant. Using the same 2D-DIC technique, the AC amplitude of vibration on the skin was measured at three test points within the measuring area, which were 1.0, 3.0, and 5.0 mm away from the contact patch, respectively.

III. Results

A. Psychophysical Experiment 1

The trajectories of one random subject in the DC-AC parameter space are shown in Fig. 6a as an example. This subject represents a general trend of consistently reaching similar gain values for the same texture within the repeated experiments, regardless of DC gains or AC gains. Across textures, the three regions of endpoints were distinct, and these endpoints were not affected by different start points.

The gain distribution for all subjects and textures is displayed in Fig. 6b. Each cross is a subject's optimal gain for a given texture, where the center of the cross is the average optimal gain and the lengths of the cross arms are the standard errors in the DC and AC direction. The 95% confidence ellipses for each texture are also shown and the centers are highlighted as squares.

To evaluate the trends of gains among all the factors, we performed a Principal Component Analysis (PCA) using two gains and three textures resulting in six entry variables. The first principal component (PC 1) accounted for 58% of the variance, and no additional components had eigenvalues larger than 1. Therefore, PC 1 can be interpreted as a "generalized gain" across gain types and textures.

A within-subjects ANOVA was also performed with factors of two types of gains and three textures to evaluate their effects on gain values. The results showed a significant effect of texture ($F(2,26) = 196.39$, $P < 0.001$), and the gains increased across texture coarseness. The effect of gain types was also significant ($F(1,13) = 265.57$, $P < 0.001$), as was the interaction ($F(1,13) = 102.10$, $P < 0.001$). On average, AC gain is greater than DC gain, but the difference is greatest for the coarsest texture (corduroy) and vanishes for the finest one (cotton).

B. Psychophysical Experiment 2

The average Likert-scale rating (from 1 to 9) of real-playback textural similarity is shown in Fig. 7. The diagonal cells represent pairs where the real texture and the playback match, and the mismatch pairs are off-diagonal. Across all texture-playback pairs, the vibration mode, stretch mode, and "both" mode had average ratings of 2.29 ± 1.19, 3.95 ± 0.41, and 5.14 ± 1.03 respectively.

A within-subject ANOVA was performed with factors of three textures and three playback modes. Only diagonal values, representing matching pairs, were used. The results indicated that the textures ($F(2,26) = 61.23$, $P < 0.001$), the playback modes ($F(2,26) = 13.97$, $P < 0.001$) and their interaction ($F(4,52) = 3.87$, $P = 0.008$) are all statistically significant. As is evident in the figure, the ratings were higher for the "both" mode, and rated similarity also increased with textural coarseness.

We further evaluated the performance of differentiating textures by comparing the diagonal and off-diagonal cells. The Receiver Operating Characteristic (ROC) curve was utilized to convert the Likert scores into discrimination measures. The ROC curves are calculated by setting a series of increasingly liberal criteria. We establish a criterion in terms of the average Likert scores to determine whether the cell indicates a match between the playback and a real texture. If the value in a cell passes the criterion and is a correct match, it is counted as a hit. Otherwise, it is a false alarm. We divided the total hits by the number of matching cases, and total false alarms by the number of non-matching cases to get the hit rate and false alarm rate. These corresponded to a point in the ROC curve space. The 1 - 9 scale was partitioned into hundredths to

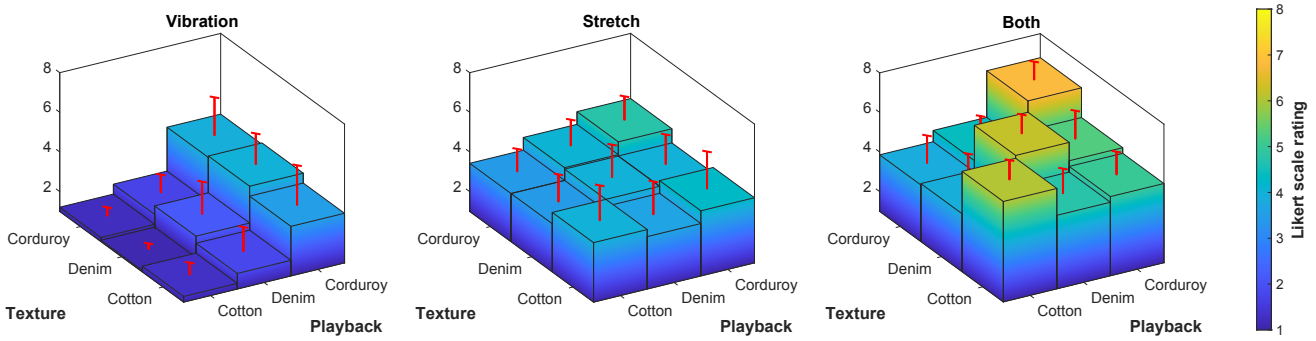

Fig. 7. 3D bar plot showing the average rating of real-playback textural similarity and the corresponding error bars. On-diagonal cells are matched textures.

build the ROC curves from the average values. The area under the ROC curve (AUC) indicates the texture discrimination measure and has a default value of 0.5. A higher value suggests a better ability for differentiation. The AUC values for vibration mode and stretch mode were 0.611 and 0.722, respectively. Since no overlaps appear between the diagonal and off-diagonal values in the "both" mode, the AUC hits the maximum possible value of 1.0 in this case. The results indicate that the "both" mode had the best performance in discriminating textures, and the stretch mode was better than the vibration mode.

C. Supplementary Experiment

A positive correlation between the DC gain and the AC amplitude is shown in Fig. 8. This result suggests that within the measurement range of this experiment, considering the same test position within the measuring area, more stretch would result in an increased amplitude of vibration, and thus, might affect skin perception. Additionally, the amplitude decreases with increasing distance from the contact patch, indicating the attenuation of vibration during propagation across the forearm skin.

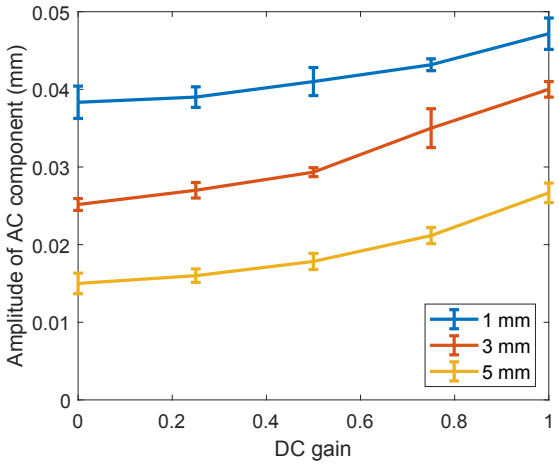

Fig. 8. DC gain versus AC amplitude at different test positions, when the vibration stimuli were the same. Error bars represent standard deviations of values from five repeated experiments.

IV. Discussion

A. Psychophysical Experiment 1

Subjects unanimously chose to scale up the DC and AC gains in order to achieve the maximum perceptual similarity between the real texture and its playback. Furthermore, the values of gains differed for each texture as seen from the three ellipses in Fig. 6b, which illustrates the individuals' variation in this 2D parameter space. The position of the three ellipses demonstrates that the spatial distribution of textures is clearly differentiated and is influenced by the topographical heights of the textures. Coarser textures (corduroy > denim > cotton) produced higher preferred gains in both DC and AC and a greater asymmetry such that AC exceeded DC.

We have also observed the consistency of gains chosen between textures for a given subject. For example, six subjects chose high AC gains for corduroy, and five of those also chose high AC gains for the other two textures. From the PCA results, most of the variability of gains could be captured by the "generalized gain" PC 1, which suggested that individual differences could be explained by sensory sensitivity, response bias, or other subject-specific factors. The variability of gains implies that a single gain pair that fits all the subjects and textures does not exist.

A similar need for increased gains during texture playback was found in a previous study [12] which examined perception via the fingertip and hypothesized that the result could be explained by the degree of engagement of RA and SA receptors *within* the contact patch. That hypothesis is supported by two recent studies with pin arrays showing that spatial variation within the fingertip contact patch increases perceived intensity [31], [32]. Such a mechanism could be at play in our work in which spatial variation within the contact patch occurred with actual textures, but not the playback device. Notably, however, our study concentrates on volar forearm skin, where the density of receptors is lower and the contact area is larger. Therefore, the same explanation may not apply. Other possible explanations are considered later based on the results of the supplementary experiment.

B. Psychophysical Experiment 2

From Fig. 7, it can be noticed that the vibration mode elicits the lowest Likert-scale scores for real-playback textural similarity, which are highly dependent on the type of

playback texture. The stretch mode evenly lifts up all the scores, but the on-diagonal and off-diagonal values are still poorly distinguishable; i.e., the subjects do not differentiate matching playbacks from those representing other textures. The combination of vibration and stretch, however, makes the scores on the diagonal higher, indicating that subjects perceived the playbacks from the "both" mode to be more similar to the corresponding textures and better differentiable from other textures.

Based on the ROC curves and associated AUC values, the stretch mode slightly outperforms the vibration mode in distinguishing diagonal values, and the "both" mode is the most effective one. A weakness of the ROC analysis is that there were only a few data points to calculate the curve. Therefore, the values of AUC should only be considered as suggestive.

It is useful to compare the AC and DC stimuli to published just-noticeable differences (JNDs). In the case of AC stimuli, the three dominant frequencies of 21 Hz, 42 Hz, and 90 Hz (see TABLE I) differ considerably more than known JNDs (e.g., [33]). This may help explain why the three different vibration mode playbacks performed quite differently (Fig. 7), although it is evident that discriminability alone did little to improve texture matching. In the case of DC stimuli, the three static stretch values of 7.3 mm, 5.7 mm, and 4.5 mm are separated by less than the JND of 4.7 mm that can be derived from [34], although that study examined lateral rather than longitudinal stretch, and compared to a reference stretch of 17.3 mm. If we consider JND in terms of Weber fraction and recall that our subjects included DC gains that were always greater than one, the differences among DC stimuli would be expected to be at or slightly above the threshold. This may help explain why the three different stretch mode playbacks performed quite similarly (Fig. 7). It is interesting, in light of DC differences being potentially less discriminable than AC, to note that the stretch mode playbacks had slightly higher AUC values than the vibration mode playbacks, further evidence that texture match requires more than supra-threshold signals.

It is particularly notable, however, that texture match improved dramatically when AC and DC inputs were combined, even though differences among the latter were approximately at threshold. Similar results have been found in other multimodal studies. For instance, [35] showed that sub-threshold visual input could enhance tactile roughness perception and discussed the extent to which central and peripheral mechanisms could explain the effect. In our case, there is little to implicate a central mechanism, but the skin stretch due to DC input has a clear impact on vibration propagation, as shown in the supplementary experiment. This is discussed next.

C. Supplementary Experiment

As seen in Fig. 8, the magnitude of vibration decays with distance from the source of the stimuli. This effect has been studied before; e.g., both Sofia and Jones [36] and Dandu *et al.* [37] have shown that vibration decays approximately exponentially with distance. Fig. 8 also shows that vibrations become stronger when the DC gain (and hence the pre-stretch of skin) increases. This phenomenon has also been reported previously [38], [39] and is perhaps related to the observation that vibration perception can be modulated by skin tension [40], [41]. Specifically, vibration sensitivity tends to be greater in "tense" skin, and weaker in loose skin. Although the connection between the physical and perceptual results has not been clearly elucidated, it stands to reason that a vibration stimulus will excite a larger population of receptors in stretched skin than in loose skin, helping subjects feel the vibration more clearly. This reasoning is further supported by related studies from Bark *et al.* [19] and Manabe *et al.* [42]. Additionally, it may explain why the ratings of the vibration mode were very low, while ratings in the "both" mode were significantly higher.

It should be noted, however, that Moore *et al.*'s work [38] also suggested that apart from decreasing the attenuation of vibration, stretch might affect the coupling of mechanoreceptors to the skin itself, thereby affecting their responses. In addition to surface waves, mechanical paths for vibration propagation could be bone conduction, tendon conduction, shear waves in the bulk, or a combination thereof [1], which are not fully considered in our discussion. Other factors that influence vibration perception might be related to the biology of the forearm skin, which varies significantly among individuals, requiring further investigation.

Future work may concentrate on understanding the necessity of stretch and vibration in the reproduction of realistic sensations. Amplified playback gains on different textures indicate that apart from mechanical factors, there might be some other missing mechanisms requiring further investigation. Although the playbacks in the second psychophysical experiment were based on the optimal gains for each subject, the original perception could not be reproduced. The results suggest that single-site uniaxial stimulation is insufficient and the smaller displacements in the other direction could play a role in creating realistic sensations such as squeezing and twisting. Another limitation of the apparatus was the use of bulk vibration on the forearm: a distributed actuator array might be able to provide texture playback with higher quality including spatial variation within the contact patch [31].

V. Conclusion

We developed an apparatus to record the mechanical responses on the skin of the volar forearm as uniaxial displacements when textures were scanned across the skin in the longitudinal direction. Dividing the displacements into DC and AC components, we reproduced the stretch and vibration of the texture scan on the same position of the forearm. Psychophysical experiments were conducted to evaluate the performance of different playback modes. The intensity of playback for each texture was adjusted by the subjects and most subjects preferred the playback to be 1 to 2 times stronger on DC components and 1 to 3.5 times stronger on AC components to obtain any perceptual similarity. It was also found that stretch and vibration patterns alone were insufficient to create differentiated textures, but a combination of both could do so. This could be explained by the fact that pre-stretched skin increased the ability of vibration to propagate

along the skin. However, the apparatus was unable to create realistic sensations of texture scans. We conclude that relying solely on single-site uniaxial displacement was inadequate for achieving realistic texture perceptibility, and other mechanisms such as multi-axis motion and spatially distributed motion could play an important role. Future work could explore the hidden mechanisms of skin stretch and vibration, and apply more complex vibration stimuli on the pre-stretched skin for texture recording and playback.

ACKNOWLEDGMENTS

This material is based upon work supported by the National Science Foundation under Grant No. 2106191. The authors would like to thank S. Tan for the use of the profilometer, and T. Trzpit for machining a part of the apparatus.

REFERENCES

[1] B. Delhaye, V. Hayward, P. Lefevre, and J.-L. Thonnard, "Texture-induced vibrations in the forearm during tactile exploration," *Front. Behav. Neurosci.*, vol. 6, 2012.

[2] L. R. Manfredi *et al.*, "Natural scenes in tactile texture," *J. Neurophysiol.*, vol. 111, no. 9, pp. 1792–1802, 2014.

[3] M. Wiertlewski, J. Lozada, E. Pissaloux, and V. Hayward, "Causality inversion in the reproduction of roughness," in *Haptics: Generating and Perceiving Tangible Sensations*. New York, NY, USA: Springer, 2010.

[4] A. Handler and D. D. Ginty, "The mechanosensory neurons of touch and their mechanisms of activation," *Nat. Rev. Neurosci.*, vol. 22, no. 9, pp. 521–537, 2021.

[5] C. E. Connor and K. O. Johnson, "Neural coding of tactile texture: comparison of spatial and temporal mechanisms for roughness perception," *J. Neurosci.*, vol. 12, no. 9, pp. 3414–3426, 1992.

[6] A. I. Weber *et al.*, "Spatial and temporal codes mediate the tactile perception of natural textures," *Proc. Nat. Acad. Sci. USA*, vol. 110, no. 42, pp. 17 107–17 112, 2013.

[7] L. Meli, I. Hussain, M. Aurilio, M. Malvezzi, M. K. O'Malley, and D. Prattichizzo, "The hBracelet: A wearable haptic device for the distributed mechanotactile stimulation of the upper limb," *IEEE Robot. Autom. Lett.*, vol. 3, no. 3, pp. 2198–2205, Jul. 2018.

[8] Y. Gaffary *et al.*, "Toward haptic communication: Tactile alphabets based on fingertip skin stretch," *IEEE Transactions on Haptics*, vol. 11, no. 4, pp. 636–645, Oct.-Dec. 2018.

[9] D. A. Mahns, N. Perkins, V. Sahai, L. Robinson, and M. J. Rowe, "Vibrotactile frequency discrimination in human hairy skin," *J. Neurophysiol.*, vol. 95, no. 3, pp. 1442–1450, 2006.

[10] M. Wiertlewski, J. Lozada, and V. Hayward, "The spatial spectrum of tangential skin displacement can encode tactual texture," *IEEE Trans. Robot.*, vol. 27, no. 3, pp. 461–472, Jun. 2011.

[11] M. Janko, R. Primerano, and Y. Visell, "On frictional forces between the finger and a textured surface during active touch," *IEEE Transactions on Haptics*, vol. 9, no. 2, pp. 221–232, Apr.-Jun. 2016.

[12] R. V. Grigorii, R. L. Klatzky, and J. E. Colgate, "Data-driven playback of natural tactile texture via broadband friction modulation," *IEEE Transactions on Haptics*, vol. 15, no. 2, pp. 429–440, Apr.-Jun. 2022.

[13] J. Wheeler, K. Bark, J. Savall, and M. Cutkosky, "Investigation of rotational skin stretch for proprioceptive feedback with application to myoelectric systems," *IEEE Trans. Neural Syst. Rehabil. Eng.*, vol. 18, no. 1, pp. 58–66, Feb. 2010.

[14] X. Yu *et al.*, "Skin-integrated wireless haptic interfaces for virtual and augmented reality," *Nature*, vol. 575, no. 7783, pp. 473–479, 2019.

[15] S. R. Williams and A. M. Okamura, "Body-mounted vibrotactile stimuli: Simultaneous display of taps on the fingertips and forearm," *IEEE Transactions on Haptics*, vol. 14, no. 2, pp. 432–444, Apr.-Jun. 2021.

[16] E. Leroy and H. Shea, "Hydraulically amplified electrostatic taxels (HAXELs) for full body haptics," *Adv. Mater. Technol.*, May 2023, Art. no. 2300242.

[17] K. Bark, J. Wheeler, P. Shull, J. Savall, and M. Cutkosky, "Rotational skin stretch feedback: A wearable haptic display for motion," *IEEE Transactions on Haptics*, vol. 3, no. 3, pp. 166–176, Jul.-Sep. 2010.

[18] J. L. Sullivan *et al.*, "Multi-sensory stimuli improve distinguishability of cutaneous haptic cues," *IEEE Transactions on Haptics*, vol. 13, no. 2, pp. 286–297, Apr.-Jun. 2020.

[19] K. Bark, J. Wheeler, S. Premakumar, and M. Cutkosky, "Comparison of skin stretch and vibrotactile stimulation for feedback of proprioceptive information," in *Proc. Symp. Haptic Interfaces Virtual Environ. Teleoperator Syst.*, 2008, pp. 71–78.

[20] D. K. Chen, I. A. Anderson, C. G. Walker, and T. F. Besier, "Lower extremity lateral skin stretch perception for haptic feedback," *IEEE Transactions on Haptics*, vol. 9, no. 1, pp. 62–68, Jan.-Mar. 2016.

[21] E. Battaglia, J. P. Clark, M. Bianchi, M. G. Catalano, A. Bicchi, and M. K. O'Malley, "Skin stretch haptic feedback to convey closure information in anthropomorphic, under-actuated upper limb soft prostheses," *IEEE Transactions on Haptics*, vol. 12, no. 4, pp. 508–520, Oct.-Dec. 2019.

[22] H. Joodaki and M. B. Panzer, "Skin mechanical properties and modeling: A review," *Proc. Inst. Mech. Eng. H: J. Eng. Med.*, vol. 232, no. 4, pp. 323–343, Apr. 2018.

[23] D. Solav *et al.*, "MultiDIC: An open-source toolbox for multi-view 3D digital image correlation," *IEEE Access*, vol. 6, pp. 30 520–30 535, May 2018.

[24] J.-T. Kim *et al.*, "Mechanics of vibrotactile sensors for applications in skin-interfaced haptic systems," *Extreme Mech. Lett.*, vol. 58, Jan. 2023, Art. no. 101940.

[25] J. P. Clark, S. Y. Kim, and M. K. O'Malley, "The rice haptic rocker: Comparing longitudinal and lateral upper-limb skin stretch perception," in *Proc. Int. Conf. Hum. Haptic Sens. Touch Enabled Comput. Appl.*, 2018, pp. 125–134.

[26] H. Olausson, J. Wessberg, and N. Kakuda, "Tactile directional sensibility: peripheral neural mechanisms in man," *Brain Res.*, vol. 866, no. 1-2, pp. 178–187, 2000.

[27] J. Biggs and M. Srinivasan, "Tangential versus normal displacements of skin: Relative effectiveness for producing tactile sensations," in *Proc. 10th Symp. Haptic Interfaces Virtual Environment Teleoperator Syst.*, 2002, pp. 121–128.

[28] H. Olausson, I. Hamadeh, P. Pakdel, and U. Norrsell, "Remarkable capacity for perception of the direction of skin pull in man," *Brain Res.*, vol. 808, no. 1, pp. 120–123, 1998.

[29] D. A. Burns, "A multi-scale, low-parameter rendering algorithm for virtual textures," Ph.D. dissertation, Northwestern Univ., Evanston, Illinois, Mar. 2023.

[30] J. A. Nelder and R. Mead, "A simplex method for function minimization," *Comput. J.*, vol. 7, no. 4, pp. 308–313, 1965.

[31] R. V. Grigorii, J. E. Colgate, and R. Klatzky, "The spatial profile of skin indentation shapes tactile perception across stimulus frequencies," *Sci. Rep.*, vol. 12, no. 1, p. 13185, 2022.

[32] Y. Massalim, D. Faux, and V. Hayward, "Distributed tactile display with dual array design," *IEEE Transactions on Haptics*, 2023.

[33] H. Pongrac, "Vibrotactile perception: examining the coding of vibrations and the just noticeable difference under various conditions," *Multimedia Syst.*, vol. 13, no. 4, pp. 297–307, 2008.

[34] Z. A. Zook, J. J. Fleck, T. W. Tjandra, and M. K. O'Malley, "Effect of interference on multi-sensory haptic perception of stretch and squeeze," in *2019 IEEE World Haptics Conference (WHC)*. IEEE, 2019, pp. 371–376.

[35] R. D. Roberts, M. Li, and H. A. Allen, "Visual effects on tactile texture perception," *Scientific Reports*, vol. 14, no. 1, p. 632, 2024.

[36] K. O. Sofia and L. Jones, "Mechanical and psychophysical studies of surface wave propagation during vibrotactile stimulation," *IEEE Transactions on Haptics*, vol. 6, no. 3, pp. 320–329, Jul.-Sep. 2013.

[37] B. Dandu, Y. Shao, A. Stanley, and Y. Visell, "Spatiotemporal haptic effects from a single actuator via spectral control of cutaneous wave propagation," in *Proc. IEEE World Haptics Conf.*, 2019, pp. 425–430.

[38] T. J. Moore, "A survey of the mechanical characteristics of skin and tissue in response to vibratory stimulation," *IEEE Trans. Man-Machine Systems*, vol. 11, no. 1, pp. 79–84, Mar. 1970.

[39] J. Pereira, J. Mansour, and B. Davis, "Dynamic measurement of the viscoelastic properties of skin," *J. Biomech.*, vol. 24, no. 2, pp. 157–162, 1991.

[40] D. Katz, *The World of Touch*. Psychology Press, 1989.

[41] B. von H. Gilmer, "The measurement of the sensitivity of the skin to mechanical vibration," *J. Gen. Psychol.*, vol. 13, no. 1, pp. 42–61, 1935.

[42] M. Manabe, K. Ushiyama, A. Takahashi, and H. Kajimoto, "Vibrotactile presentation using a motor within a housing and rotor fixed to the skin," in *Proc. IEEE World Haptics Conf.*, 2021, pp. 906–911.

Zhenyu Liu received the B.Eng. degree in mechanical engineering from Zhejiang University, Hangzhou, China, in 2021, and the M.S. degree in mechanical engineering from Northwestern University, Evanston, IL, USA, in 2023. His current research interests include haptics interfaces and tactile perception.

Jin-Tae Kim received the B.S. degree in mechanical engineering from Oklahoma State University, Stillwater, OK, USA, in 2013, and the M.S. and Ph.D. degrees in theoretical applied mechanics from the University of Illinois at Urbana-Champaign, Urbana, IL, USA, in 2015 and 2020, respectively. He is currently a postdoctoral researcher at the Querrey Simpson Institute for Bioelectronics, Northwestern University, Evanston, IL, USA, and an adjunct assistant professor with a joint appointment at the Pohang University of Science and Technology, Pohang, South Korea.

John A. Rogers (Fellow, IEEE) began his career at Bell Laboratories in the Condensed Matter Physics Research Department in 1997, and served as Director from the end of 2000 to 2002. He then spent thirteen years at the University of Illinois, as the Swanlund Chair Professor and Director of the Seitz Materials Research Laboratory. In 2016, he joined Northwestern University as the Simpson/Querrey Professor of Materials Science and Engineering, Biomedical Engineering and Medicine, where he is also Director of the Institute for Bioelectronics. He is a member of the National Academy of Engineering, the National Academy of Sciences and the National Academy of Medicine.

Roberta L. Klatzky (Fellow, IEEE) received the Ph.D. degree in cognitive psychology from Stanford University. She is the Charles J. Queenan, Jr. University Professor at Carnegie Mellon University, Pittsburgh, PA, USA, where she is a member of the Department of Psychology, Human–Computer Interaction Institute, and Neuroscience Institute. Her research interests include human perception and cognition, with special emphasis on spatial cognition and haptic perception.

J. Edward Colgate (Fellow, IEEE) is the Walter P. Murphy professor of mechanical engineering at Northwestern University, Evanston, IL, USA. His principal research interests include haptic interfaces and human-robot interaction. Dr. Colgate was the founding Editor-in-Chief of the IEEE Transactions on Haptics. He is a Fellow of the National Academy of Inventors, and a Member of the National Academy of Engineering. He and collaborator Michael Peshkin are the inventors of cobots, which led to their first startup together, Cobotics Inc. Their second startup, Kinea Design, developed advanced physical therapy robots and prosthetic limbs. Their third company together, Tanvas Inc., commercialized innovative surface haptic technologies that allow users to feel tactile effects on a touch screen.